Available online at website: https://journal.bcrec.id/index.php/bcrec

Bulletin of Chemical Reaction Engineering & Catalysis, 20 (4) 2025, 640-649

Original Research Article

Green Synthesis of Cu-BDC Nanosheet for Methylene Blue Degradation

Nanda Saridewi[1,2], Agustino Zulys[1*], Ridla Bakri[1]

[1]Department of Chemistry, Faculty of Mathematics and Natural Sciences, University of Indonesia, Jl. Lingkar Kampus Raya, Pondok Cina, Beji, Depok, Jawa Barat 16424, Indonesia.
[2]Department of Chemistry Education, Faculty of Tarbiya and Teaching Sciences, UIN Syarif Hidayatullah, Jl. Ir. H. Juanda No. 95, Ciputat Tangerang Selatan 15412, Indonesia.

Received: 30th July 2025; Revised: 15th September 2025; Accepted: 16th September 2025
Available online: 22th September 2025; Published regularly: December 2025

Abstract

Metal Organic Frameworks (MOFs) with two-dimensional (2D) nanosheet morphology possess unique surface characteristics, making them highly favourable for photocatalytic applications. This study synthesised Cu^{2+}-based MOF nanosheets using a modified three-layer method. This approach is relatively simple, energy-efficient, and qualifies as a green synthesis method. The MOFs were prepared from copper(II) nitrate trihydrate ($Cu(NO_3)_2 \cdot 3H_2O$) as the metal precursor and 1,4-benzenedicarboxylic acid (H_2BDC) as the organic linker, aiming to evaluate their photocatalytic activity for methylene blue degradation. The resulting Cu-BDC nanosheets displayed characteristic FTIR absorption bands at 1501 and 1547 cm^{-1} corresponding to symmetric and asymmetric C=O stretching, 1394 cm^{-1} for C–O stretching, and peaks at 751 and 569 cm^{-1} associated with Cu–O vibrations. The XRD analysis revealed four sharp peaks at 2θ values of 8.2°, 10.2°, 16.1°, and 34.1°, indicating good crystallinity with a calculated crystallite size of 22.03 nm, and the bandgap energy is 3.89 eV. Cu-BDC nanosheets exhibit a thin sheet morphology with elemental compositions of carbon 73.08%, oxygen 11.19%, and copper 15.73%. Cu-BDC nanosheets exhibit optimal degradation activity at pH 13, with an optimal catalyst dose of 5 mg and an initial dye concentration of 20 ppm, achieving a degradation capacity of 98.62 mg/g after 120 minutes of reaction.

Keywords: Green synthesis; methylene blue; Cu-BDC nanosheet; Metal Organic Frameworks; MOFs

How to Cite: Saridewi, N., Zulys, A., Bakri, R. (2025). Green Synthesis of Cu-BDC Nanosheets for Methylene Blue Degradation. *Bulletin of Chemical Reaction Engineering & Catalysis*, 20 (4), 640-649. (doi: 10.9767/bcrec.20458)

Permalink/DOI: https://doi.org/10.9767/bcrec.20458

1. Introduction

Environmental issues, notably water pollution, have significantly impacted human life and health [1]. One of the leading causes of this pollution is the rapid growth of the industrial sector, which has not been matched by adequate waste treatment systems. Liquid waste discharged directly into the environment without proper treatment, especially from the textile, plastic, paper, and pulp industries, often contains harmful organic dyes that are difficult to break down naturally [2]. One example of such dye waste is methylene blue, which is widely used in the textile industry and can cause serious environmental problems if not properly managed.

To address this issue, one rapidly developing method is photocatalysis, a technique for degrading organic compounds using semiconductor materials and light energy, either from UV rays or visible light. This method is considered a promising alternative solution because it can selectively break down pollutants into simpler compounds with high efficiency [3]. Additionally, photocatalysis is environmentally

* Corresponding Author.
Email: zulys@ui.ac.id (A. Zulys)

friendly, energy-efficient, and chemical-free [4], and does not require further processing of the degradation products [5].

Metal organic frameworks (MOFs) have been widely reported to be successfully used in photocatalysis, including in the degradation of organic pollutants [5], CO2 reduction [6], and water splitting for hydrogen gas production [7]. MOFs can act as semiconductors due to their ability to absorb photons from light and their high porosity [8]. The pores of MOFs are sufficiently large, making them better catalysts than metal oxides [9].

Metal–Organic Frameworks (MOFs) offer distinct advantages over conventional semiconductor materials, particularly their structural tunability. By varying the organic ligands and metal ions, MOFs can be engineered to exhibit diverse structures with tailored physical and chemical properties [10–11]. However, ongoing research has revealed several limitations. For instance, exposure to humidity can reduce their surface area and adsorption capacity. Additionally, certain MOFs suffer from low electrical conductivity and limited pore sizes, which hinder efficient gas diffusion.

Various modification strategies have been explored to overcome these challenges. One promising approach involves tailoring the morphology or dimensionality of MOFs. Specifically, MOFs can be synthesised in two-dimensional (2D) forms, known as nanosheets, which consist of ultra-thin layers with nanometer-scale thicknesses [12–17]. These 2D MOF nanosheets offer improved accessibility to active sites and enhanced charge transport properties, making them attractive for applications such as catalysis and sensing.

Nanosheets are porous carbon structures in thin sheets at the nanometer scale with a very high surface area. This enables them to hold large amounts of electrostatic charge and produce superior capacitive properties. In addition, the space between the sheets provides an efficient ion transport pathway, ultimately contributing to improved energy storage performance [18].

The solvothermal method, a bottom-up approach, is one of the most commonly used synthesis techniques in producing metal-organic frameworks (MOFs), including for the formation of nanosheet structures [19]. The synthesis of MOF nanosheets can be carried out with modulators [20] or surfactants [21] as crystal growth controllers. However, the synthesis of MOF nanosheets remains a significant challenge, as it requires exact control of crystal growth to ensure that formation occurs only in the vertical direction (thickness). In contrast, the lateral direction is maintained at the two-dimensional scale.

The three-layer method is an alternative synthesis approach that leverages interfacial density differences to facilitate MOF formation [22]. This practical and environmentally friendly technique eliminates the need for high energy input and excessive chemical usage. Its simplicity, low environmental impact, and resource efficiency make it well-suited for green synthesis applications [23].

This study therefore aimed to modify the three-layer synthesis method by combining two solvents with significant density differences and adapting the stirring technique to produce Cu-BDC nanosheets more efficiently and sustainably. The approach combines solvent density differences and controlled stirring to enhance nanosheet formation and catalytic activity, offering a simple, cost-effective, and environmentally friendly strategy. It also explores the potential of copper-based MOFs, which are less studied, for photocatalytic degradation of organic dyes. Copper was chosen due to its advantageous electronic properties, including high d-orbital occupancy and a partially filled d-orbital configuration, contributing to its effective catalytic performance [24]. Moreover, copper is a widely available transition metal and is more cost-effective than many other transition metals [25–28]. The synthesized Cu-BDC nanosheets were then evaluated for their photocatalytic performance in degrading methylene blue, providing insight into the potential application of copper-based MOFs for the treatment of organic dye pollutants.

2. Materials and Method

2.1 Materials

The materials used in this study include: 1,4-benzenedicarboxylic acid (H_2BDC) emsure grade p.a (Sigma Aldrich), copper (II) nitrate trihydrate ($Cu(NO_3)_2.3H_2O$) emsure grade p.a (Supelco), distilled water, sodium hydroxide (NaOH) emsure grade p.a (Merck), ethanol 96%, N,N-dimethylformamide (DMF) emsure grade p.a (Pallav), acetonitrile emsure grade p.a (Merck), and methylene blue emsure grade p.a (Merck).

2.2 Synthesis of Cu-BDC Nanosheet

Copper(II) nitrate trihydrate ($Cu(NO_3)_2 \cdot 3H_2O$) (3.725 mmol) was dissolved in a 120 mL of solvent mixture of N,N-dimethylformamide (DMF) and acetonitrile (3:1 v/v). The organic linker 1,4-benzenedicarboxylic acid (H_2BDC) (0.02 mmol) was dissolved in the 120 mL of solvent mixture of N,N-dimethylformamide (DMF) and acetonitrile (1:3 v/v). The H_2BDC solution was then dropwise to the copper solution under continuous stirring to ensure homogeneous mixing and coordination.

The mixture was stirred for 24 h at room temperature, followed by a static ageing process for 7 days to facilitate nanosheet formation. The synthesised Cu-BDC nanosheets were subsequently collected by centrifugation, washed, filtered, and dried.

2.3 Characterization of Cu-BDC Nanosheet

Functional group analysis was conducted using a Prestige 21 Fourier Transform Infrared (FTIR) spectrophotometer at room temperature, with a scanning range of 400–4000 cm^{-1} and a spectral resolution of 4 cm^{-1}. Potassium bromide (KBr) powder was used as the background reference. X-ray diffraction (XRD) was performed using Shimadzu XRD-7000 Maxima with monochromatic Cu Kα radiation (λ = 1.54056 Å) at 30 mA and 40 kV. Diffractograms were analyzed using Origin software to determine crystallite size, crystallinity, and phase type. Crystal size was calculated using the Debye-Scherrer equation (Eq. 1):

$$D = \frac{k\lambda}{\beta \cos\theta} \quad (1)$$

where D is crystal size, k = 0.9, λ = 1.5418 Å, β is FWHM (rad), and θ is diffraction angle (°).

The surface morphology of Cu-MOFs nanosheets was examined using FESEM TFS Apreo 2S, which acquired images at a voltage of 2 kV (SE and BSE). The 2D structure of Cu-MOFs was analysed using Transmission Electron Microscopy (TEM), FEI Talos F200X at an acceleration voltage of 200 kV, HAADF-STEM mode, and EDS for elemental composition analysis.

UV-Vis diffuse reflectance spectroscopy (DRS) was conducted a Thermo-Scientific Genesys 10s UV-Vis at the 200–800 nm range using $BaSO_4$ as a reference. Band gap energy was estimated using the Kubelka–Munk function (Eq. 2):

$$F(R) = \frac{(1-R)^2}{2R} \quad (2)$$

The band gap was further determined using the Tauc relation (Eq. 3), where $ahv = A(hv - E_g)^n$ with n = ½ for direct and 2 for indirect transitions. By substituting $F(R) \approx \alpha$ (Eq. 4), a plot of $[F(R)hv]^{1/n}$ versus hv was used to determine E_g from the x-intercept of the linear region.

$$\alpha(hv) \approx A\left(hv - E_g\right)^n \quad (3)$$

$$[F(R)hv]^{1/n} = A\left(hv - E_g\right) \quad (4)$$

2.4 Photocatalytic Activity Test of Cu-BDC Nanosheets

10 mg of Cu-BDC nanosheets was dispersed into 50 mL of methylene blue (5 ppm). The mixture was stirred at 300 rpm at room temperature for 2 hours in the dark and under visible light (250-watt mercury lamp). Then, 2 mL of the suspension was taken every 30 minutes for 2 h and centrifuged at 6000 rpm for 10 minutes. The absorbance of methylene blue was measured using a UV-Vis spectrophotometer at a wavelength of 665 nm. The following Eq. 5-6 determined the degradation efficiency and degradation capacity of methylene blue.

$$DE\ (\%) = \frac{(C_0 - C_t)}{C_0} \times 100\% \quad (5)$$

$$Q\ \left(\frac{mg}{g}\right) = \%\ Degradation\ \times\ C_0\ \times \frac{V}{m} \quad (6)$$

Where C_0 is initial concentration of methylene blue (mg/L) (t = 0 min), C_t is methylene blue concentration at a certain reaction time, DE is degradation efficiency (%), Q is degradation capacity (mg/g), m is mass of photocatalyst (g), and V is methylene blue solution volume (L).

3. Results and Discussion

3.1 Cu-BDC Nanosheets

In this study, the synthesis of Cu-BDC nanosheets was conducted using a bottom-up approach via a modified three-layer technique. This method is based on the principle of controlled crystal growth by reducing both diffusion and nucleation rates, thereby enabling the formation of well-defined nanosheet structures [28]. The technique involves using two immiscible solvents with significantly different densities, where the less dense solvent is layered on top of the denser one. An optional buffer layer—typically a mixture of the two solvents in equal proportions—can be introduced between them to moderate the interface and control diffusion more precisely.

A similar approach was reported by researcher [27], who applied the three-layer method with slight modifications to synthesise Cu-BDC nanosheets. In their study, the top layer consisted predominantly of acetone (low density), the bottom layer was rich in DMF (high density), and the middle layer contained a 1:1 mixture of acetone and DMF. The solvent layering formed a stable vertical gradient, promoting controlled diffusion and orderly crystal formation. In contrast, Shete *et al.* [22] employed a simpler approach by directly mixing the metal and ligand solutions in a single container. They allowed the reaction to proceed under static conditions for 24 hours at room temperature, followed by shaking at various temperatures.

This study employs a green synthesis approach, utilising room temperature and simple equipment. To prepare the metal solution, this procedure dissolves copper salt in a mixture of

acetonitrile (CH_3CN) and DMF solvents. Simultaneously, this process dissolves H_2BDC in a CH_3CN: DMF mixture with a 1:3 ratio to form the ligand solution. The solvents' significant density difference slows the diffusion process, promoting gradual crystal growth. The result shows that the system forms thin MOF nano sheets after being undisturbed for 7 days, as shown in Figure 1. The uniform colour of the resulting material indicates a complete reaction, with no residual copper salts or BDC ligands from the initial synthesis mixture.

3.2 Characteristics of Cu-BDC Nanosheets

3.2.1 Functional group

Figure 2 displays the FTIR absorption peaks corresponding to the functional groups present in the Cu-BDC nanosheets. The broad band at 3438 cm^{-1} arises from crystalline water [29] or hydroxyl groups (–OH) associated with the carboxylic acid (–COOH) [30]. The peaks at 1501 and 1547 cm^{-1} represent the symmetric and asymmetric stretching vibrations of the C=O groups, while the peak at 1394 cm^{-1} corresponds to the C–O stretching vibration. These results align with the findings reported by [31], who observed similar bands for symmetric and asymmetric C=O stretching and C–O stretching at 1507, 1613, and 1392 cm^{-1}, respectively. In the fingerprint region, the 751 and 569 cm^{-1} peaks indicate Cu–O bond vibrations, confirming the BDC linker's coordination between Cu^{2+} ions and the carboxylate groups.

3.2.2 Crystallinity and crystal size of Cu-BDC nanosheets

The XRD pattern of the synthesised Cu-BDC nanosheets (Figure 3) reveals three sharp and intense diffraction peaks at 2θ = 10.2°, 16.9°, and 34.1°, closely resembling the pattern reported by Shete *et al.* [32]. This similarity confirms the successful formation of Cu-BDC nanosheets structures. The sharp and narrow peaks observed in the XRD analysis also indicate that the Cu-BDC nanosheets exhibit high crystallinity [33].

Using the Debye–Scherrer equation, the calculated crystallite size of the Cu-BDC nanosheets was 22.03 nm. This value is smaller than those reported in other studies for bulk Cu-BDC, which range from 22.18 nm [34] to 67.96 nm [35] and 28 nm [36]. The smaller crystal size suggests a larger surface area, which enhances the photocatalytic efficiency of the material in dye degradation applications [37].

The successful formation of highly crystalline Cu-BDC nanosheets highlights the effectiveness of the green synthesis approach in this work. The small crystal size also implies fewer structural defects, further supporting the quality of the resulting MOF. The slow and controlled crystal growth achieved through this method plays a crucial role in tailoring both the size and morphology of the Cu-BDC nanosheets [27].

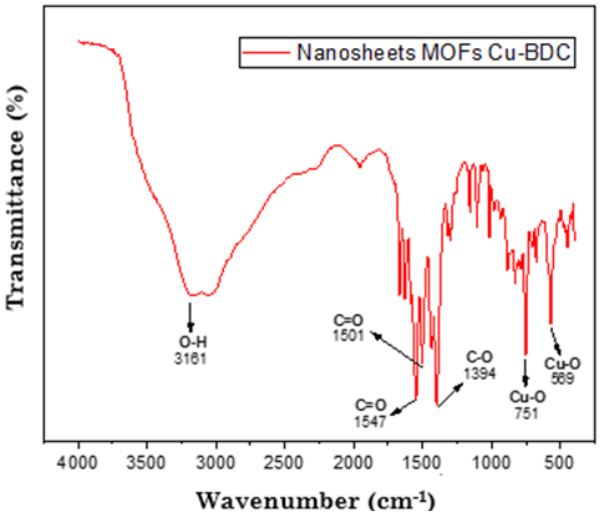

Figure 2. FTIR spectra of Cu-BDC nanosheets.

Figure 1. Cu-BDC MOF nanosheets.

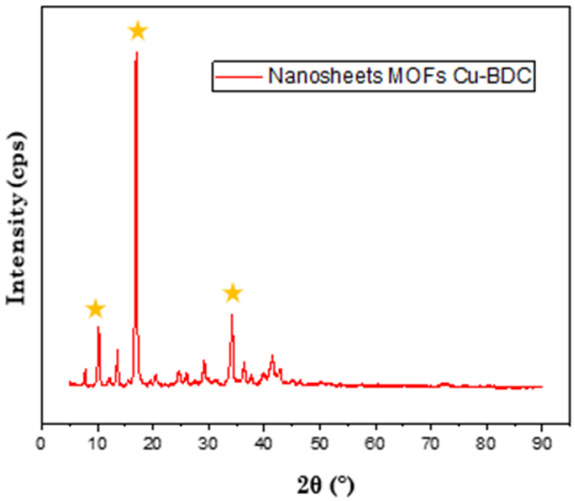

Figure 3. Diffraction patterns of Cu-BDC nanosheets.

3.2.3 Band gap energy of Cu-BDC nanosheet

The band gap energy of Cu-BDC nanosheets is 3.89 eV (Figure 4). Other studies on bulk Cu-BDC nanosheets reported band gap energies of 3.79 eV [38] and 3.62 eV [39]. This indicates that Cu-BDC nanosheets' morphology can influence the MOF material's band gap energy.

3.2.4 Morphology of Cu-BDC nanosheets

The morphology of Cu-BDC nanosheets was obtained from FESEM and STEM characterization results. The desired thin sheets from this synthesis process can be seen in Figures 5 and 6. The morphology of the synthesized Cu-BDC nanosheets exhibits thin, sheet-like structures with nanometer-scale thickness, as shown in Figure 5a. This morphology confirms the successful formation of two-dimensional nanosheets [29,40]. FESEM analysis further reveals the presence of square-shaped lateral sheets with an average surface area of approximately 2 µm (Figure 5b), consistent with the findings of Shete *et al.* who reported lateral dimensions of around 2.5 µm [27].

STEM analysis provides a more precise visualization of the nanosheet morphology, displaying ultrathin, square-like sheets with well-defined edges (Figure 6a–c). Elemental mapping confirms the uniform distribution of copper (Cu), oxygen (O), and carbon (C) across the sheets (Figure 6d). Zhan *et al.* also observed a similar lamellar structure in Cu-BDC nanosheets using HAADF-STEM, characterized by a rectangular morphology with dimensions of approximately 300 nm [32]. These results demonstrate that the employed synthesis strategy effectively produces two-dimensional MOF nanosheets with vertically oriented planes and well-preserved structural integrity.

The elemental composition of the Cu-BDC nanosheets, summarized in Table 1, shows that copper ions—serving as metal nodes—constitute 15.73% of the material. This percentage is notably higher than the 10.97% Cu content reported by Dastbaz et al. for similar nanosheets [40]. The dominant carbon content arises from the BDC ligands acting as organic linkers in the MOF framework. These findings confirm the successful assembly of Cu-BDC nanosheets composed of well-coordinated copper ions and BDC linkers.

3.3 Photocatalytic Activity of Cu-BDC Nanosheets

Preliminary tests under dark and light conditions under visible light were conducted with a methylene blue concentration of 5 ppm at pH of 11 using 5 mg of Cu-BDC nanosheets. The methylene blue degradation efficiency by Cu-BDC

Table 1. Composition of Cu-BDC nanosheets.

No.	Element	Composistion (%)
1.	Carbon (C)	73.08
2.	Oxygen (O)	11.19
3.	Copper (Cu)	15.73

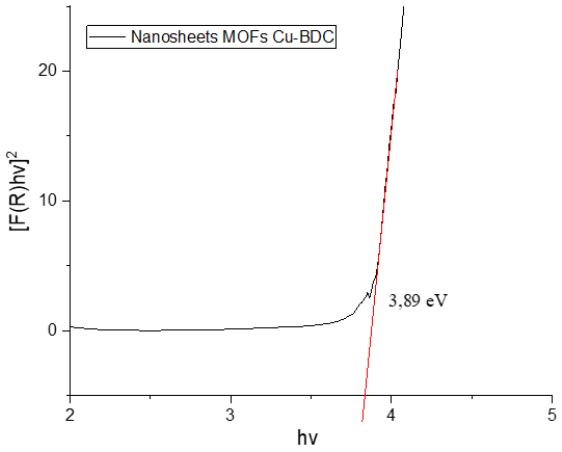

Figure 4. Energy gap of Cu-BDC nanosheets.

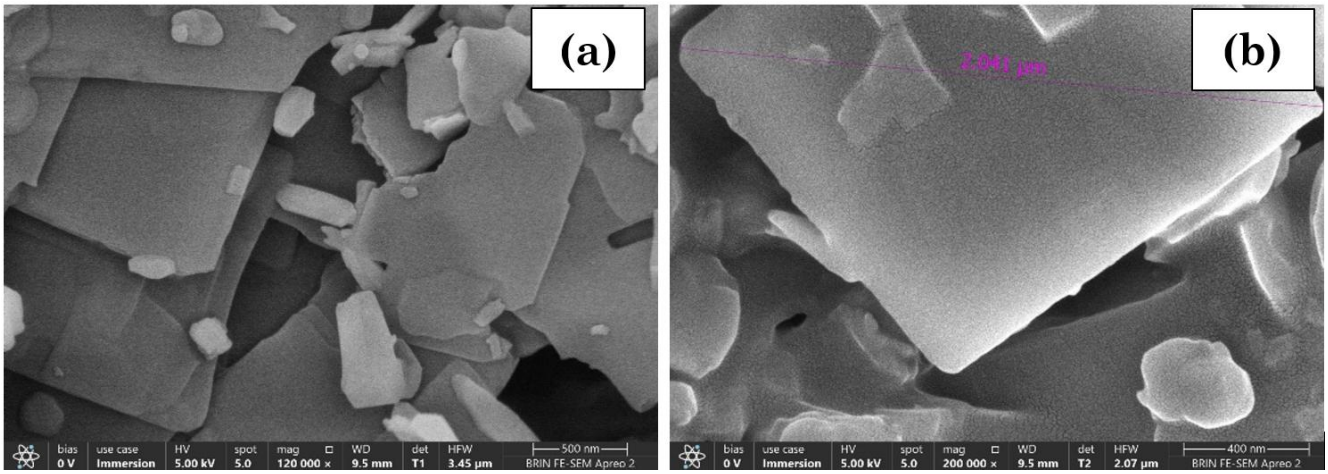

Figure 5. FESEM morphology of Cu-BDC nanosheets.

nanosheets under dark conditions was 49.731%, while it was 93.544% under light conditions. The degradation capacity under light conditions also obtained higher results, namely 23.417 mg/g, while it was 12.203 mg/g under dark conditions. This indicates that the photocatalysis of methylene blue by Cu-BDC MOF nanosheets has occurred. The difference in efficiency and degradation percentages between light and dark reactions indicates that light has aided the degradation of methylene blue (photodegradation). Photon energy exposes the photocatalyst to generate excited electrons in the conduction band and electron holes (h^+) in the valence band. The excited electrons react with oxygen molecules bound to the photocatalyst surface to form superoxide radical anions ($\cdot O_2^-$). These anions react with water molecules (H_2O) adsorbed on the photocatalyst surface to produce hydroxide ions (OH^-), which then react with electron holes (h^+) to form $OH\cdot$ radicals, which are strong oxidisers for dye degradation. On the other hand, h^+ reacts with water molecules (H_2O) to form hydroxyl radicals ($OH\cdot$), which subsequently degrade the blue methylene compound into CO_2 and H_2O [41-42].

Cu-BTC nanosheets exhibit significant photocatalytic activity due to a combination of their structural and electronic properties. The 2D structure of the nanosheets increases the specific surface area, providing more active sites for interaction with target molecules, while also facilitating the diffusion of compounds into the material's pores. Cu^{2+} ions in the MOF framework act as active centers that facilitate electron transfer when the material is excited by visible light, generating electron-hole pairs (e^-/h^+) that subsequently form reactive radicals such as $\cdot OH$

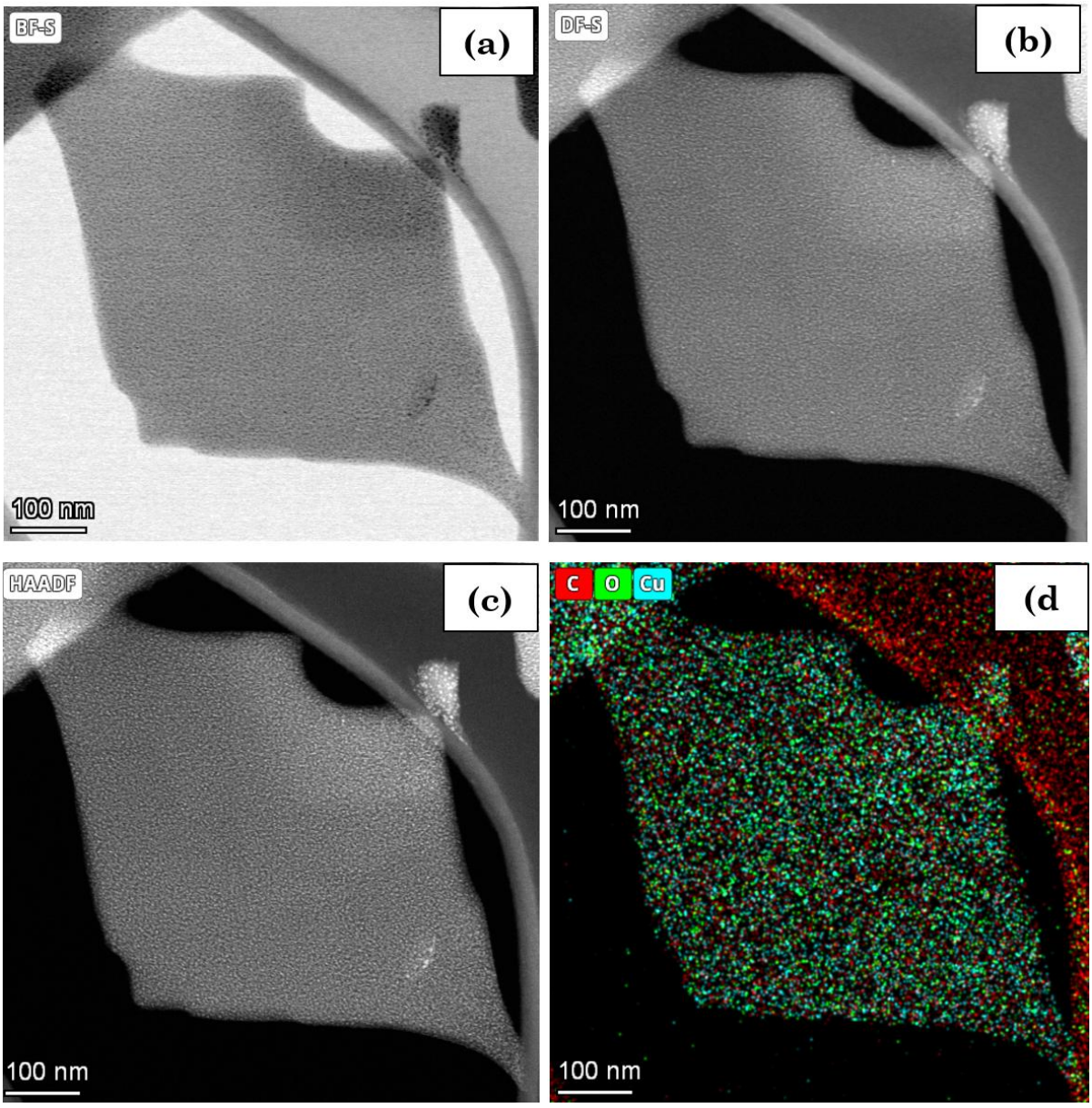

Figure 6. Results of STEM analysis of Cu-BDC nanosheets.

and $\cdot O_2^-$. These radicals are responsible for the degradation of organic compounds, such as methylene blue. Furthermore, the thin nanosheet morphology reduces the electron diffusion distance, thereby decreasing electron-hole recombination and enhancing photocatalytic efficiency.

3.4 Effect of Methylene Blue Concentration

The degradation efficiency increased significantly at methylene blue concentrations of 5 to 15 ppm, namely 93.544, 81.348, and 57.069%, while at a concentration of 20 ppm, there was a decrease of 55.896%. Degradation capacity increased with increasing methylene blue concentration, reaching 23.417, 39.413, 40.073, and 57.223 mg/g. The highest degradation efficiency was achieved at a methylene blue concentration of 5 ppm, with a degradation efficiency of 93.544% and a degradation capacity of 23.417 mg/g. Optimal conditions were obtained at a methylene blue concentration of 20 ppm, with a degradation efficiency of 55.896% and a degradation capacity of 57.223 mg/g.

Hayu *et al*. found that the higher the concentration of methylene blue, the lower the degradation capacity [43–44]. According to Hevira et al., at low initial dye concentrations, the active sites on the photocatalyst are sufficient to adsorb a certain amount of dye, resulting in high degradation efficiency but low degradation capacity due to the low dye concentration [45]. Chen & Mao stated that this could occur because the photocatalyst had reached a saturated phase where high dye concentrations covered the surface, reducing photon efficiency and deactivation [46]. In contrast to this study, the degradation capacity continues to increase even when the dye concentration increases. The morphology of the catalyst influences this. Thin sheets with large widths allow the catalyst to provide numerous active sites to support the catalytic process. Therefore, transforming bulk material into two-dimensional material is highly advantageous for applications [40].

3.5 Effect of Cu-BDC Nanosheets Mass

The degradation efficiency decreased markedly with increasing photocatalyst mass from 5 to 20 mg, with values of 41.680%, 37.049%, 34.745%, and 31.749%, respectively. Similarly, the degradation capacity declined significantly, from 85.752 mg/g at 5 mg catalyst mass to 37.929, 23.637, and 16.408 mg/g at higher catalyst loadings. The optimal photocatalytic performance was achieved at a Cu-BDC nanosheets mass of 5 mg, yielding a degradation efficiency of 41.680% and a degradation capacity of 85.752 mg/g.

As the catalyst mass increased, both degradation efficiency and capacity consistently declined. This trend aligns with the findings of Adawiah *et al*. [47], who reported that the highest photocatalytic activity occurred at the lowest catalyst mass. The decrease in performance at higher catalyst concentrations is attributed to the increased density of solid particles in the reaction system, which scatters and blocks incident light, thereby reducing the activation of photocatalyst surfaces during the photodegradation process [48].

3.6 Effect of pH

The degradation efficiency value increased significantly with increasing pH of methylene blue from 9 to 13, namely 29.800; 38.524; 41.680; 45.992; and 49.032%. Degradation capacity also showed a significant increase with increasing pH of methylene blue, reaching 61.016, 78.496, 85.752, 92.348, and 98.615 mg/g. Optimal conditions were achieved at a methylene blue pH of 13, with a degradation efficiency of 49.032% and a degradation capacity of 98.615 mg/g after 120 minutes of reaction. The reaction conditions were only conducted at basic pH because the Cu-BDC nanosheets did not exhibit catalytic activity at acidic pH. Under basic conditions, Cu-BDC nanosheets become negatively charged. This leads to strong interactions with methylene blue, a cationic dye [49]. An increase in the number of OH^- ions at basic pH also increases the number of $\cdot OH$, thereby enhancing the photodegradation process of methylene blue dye [50].

4. Conclusions

Cu-BDC nanosheets were successfully synthesised and characterised, exhibiting ultra-thin sheet morphology based on FESEM and STEM analysis. The elemental composition consisting of C (73.08%), O (11.19%), and Cu (15.73%) supports the characteristic structure of Cu-BDC nanosheets. Photocatalytic testing using methylene blue confirmed the higher photocatalytic activity of the nanosheets under illumination. Optimal conditions were obtained at pH 13 with a catalyst mass of 5 mg and a dye concentration of 20 ppm, yielding a degradation efficiency of 49.03% and a degradation capacity of 98.62 mg/g after 120 minutes of reaction. These results indicate that this simple and environmentally friendly synthesis method effectively produces Cu-BDC nanosheets with good photocatalytic performance.

CRedit Author Statement

Author Contributions: N. Saridewi: conceptualization, investigation, methodology, data curation, formal analysis, writing an original draft; A. Zulys: Supervision, research design, conceptualization, and writing - review & editing;

R. Bakri: Supervision. All authors have read and agreed to the published version of the manuscript.

Declaration of Competing Interest

The authors declare that they have no known competing financial interests or personal relationships that could have appeared to influence the work reported in this paper.

References

[1] Nguyen, V.Q., Mady, A.H., Mahadadalkar, M.A., Baynosa, M.L., Kumar, D.R., Rabie, A.M., Lee, J., Kim, W.K., Shim, J.J. (2022). Highly active Z-scheme heterojunction photocatalyst of anatase TiO2 octahedra covered with C-MoS2 nanosheets for efficient degradation of organic pollutants under solar light. *J. Colloid Interface Sci*., 606, 33752. DOI: 10.1016/j.jcis.2021.07.128

[2] Wu, Y.H., Wu, T., Lin, Y.W. (2019). Photoelectrocatalytic degradation of methylene blue on cadmium sulfide–sensitized titanium dioxide film. *Mater. Res. Bull*., 118, 110500. DOI: 10.1016/j.materresbull.2019.110500

[3] Khan, S., Noor, T., Iqbal, N., Yaqoob, L. (2024). Photocatalytic dye degradation from textile wastewater: a review. *ACS Omega*, 9(20), 21751–21767. DOI: 10.1021/acsomega.4c00887

[4] Naimah, S., Ardhanie, S.A., Jati, B.N., Aidha, N.N., Arianita, A.C. (2014). Degradasi Zat warna pada limbah cair industri tekstil dengan metode fotokatalitik menggunakan nanokomposit TiO2-Zeolit. *Jurnal Kimia Kemasan*, 36(2), 225–236. DOI: 10.24817/jkk.v36i2.1889

[5] Roy, S., Darabdhara, J., Ahmaruzzaman, Md. (2024). Recent advances of Copper- BTC metal-organic frameworks for efficient degradation of organic dye-polluted wastewater: synthesis, mechanistic insights and future outlook. *Journal of Hazardous Materials Letters*, 5(4), 1–10. DOI: 10.1016/j.hazl.2023.100094

[6] Chen, Y., Wang, D., Deng, X., Li, Z. (2017). Metal–organic frameworks (MOFs) for photocatalytic CO2 reduction. *Catalysis Science Technology*, 7 (21), 4893–4904. DOI: 10.1039/C7CY01653K

[7] Nguyen, H.L. (2021). Metal–organic frameworks for photocatalytic water splitting. *Solar RRL*, 5(7), 1–19. DOI: 10.1002/solr.202100198

[8] Hidayat, R., Saputra, A., Fitria, M. (2022). Material MOFs (metal organic frameworks) dalam aplikasi fotokatalisis: mini review. *IJCA (Indonesian Journal of Chemical Analysis)*, 5(2), 120–137. DOI: 10.20885/ijca.vol5.iss2.art7

[9] Gautam, S., Agrawal, H., Thakur, M., Akbari, A., Sharda, H., Kaur, R., Amini, M. (2020). Metal oxides and metal organic frameworks for the photocatalytic degradation: a review. *Journal of Environmental Chemical Engineering*, 8(3), 1–15. DOI: 10.1016/j.jece.2020.103726

[10] Cao, X., Tan, C., Sindoro, M., Zhang, H. (2017). Hybrid micro-/nano-structures derived from metal–organic frameworks: preparation and applications in energy storage and conversion. *Chem. Soc. Rev*., 46, 2660–2677. DOI: 10.1039/C6CS00426A

[11] Li, N., Li, H., Ji, R., Lin, S., Xu, C., Huang, J., Zhou, Q., Lyu, S., Li, F., Tang, J. (2023). Fabrication of bimetallic MOF with 2D nanosheets structure and rich active sites for enhanced removal of organic pollutants by activation of peroxymonosulfate. *Journal of Environmental Chemical Engineering*. 2023, 11, 110607. DOI: 10.1016/j.jece.2023.110607

[12] Zhao, K., Zhu, W., Liu, S., Wei, X., Ye, G., Su, Y., He, Z. (2020). Two-dimensional metal–organic frameworks and their derivatives for electrochemical energy storage and electrocatalysis. *Nanoscale Advances*. 2, 536. DOI: 10.1039/C9NA00719A

[13] Solomos, M.A., Clairea, J., Kempa, T.J. (20190. 2D molecular crystal lattices: advances in their synthesis, characterization, and application. *Journal of Materials Chemistry A*. 7, 25537. DOI: 10.1039/C9TA06534B

[14] Khan, S., Shahid, M. (2021). Throwing light on the current developments of two-dimensional metal–organic framework nanosheets (2D MONs). *Materials Advances*. 2, 4914. DOI: 10.1039/D1MA00389E

[15] Wang, X., Chi, C., Zhang, K., Qian, Y., Gupta, K. M., Kang, Z., Jiang, J., Zhao, D. (2017). Reversed thermo-switchable molecular sieving membranes composed of two-dimensional metal-organic nanosheets for gas separation. *Nat. Commun.*, 2017, 8, 1–10. DOI: 10.1038/ncomms14460

[16] Carne´, A., Carbonell, C., Imaz, I., Maspoch, D. (2011). Nanoscale metal–organic materials. *Chem. Soc. Rev*., 2011, 40, 291–305. DOI: 10.1039/C0CS00042F

[17] Rocca, V. D., Liu, D., Lin, W. (2011). Nanoscale metal-organic frameworks for biomedical imaging and drug delivery. *Acc. Chem. Res*., 2011, 44, 957–968. DOI: 10.1021/ar200028a

[18] Li, Z.X., Yang, B.L., Zou, K.Y., Kong, L., Yue, M.L., Duan H.H. (2018). Novel porous carbon nanosheet derived from a 2D Cu-MOF: Ultrahigh porosity and excellent performances in the supercapacitor cell. *Carbon*. 2018, 144, 540-54. DOI: 10.1016/j.carbon.2018.12.061

[19] Yu, Y.H., Lin, X.Y., Teng, K.L., Lai, W.F., Hu, C.C., Tsai, C.H., Liu, C.P., Lee, H.L., Su, C.H., Liu, Y.H., Lu, K.L., Chien, S.Y. (2023). Synthesis of two-dimensional (Cu–S)n metal–organic framework nanosheets applied as peroxidase mimics for detection of glutathione. *Inorg. Chem*. 62, 42, 17126–17135. DOI: 10.1021/acs.inorgchem.3c02023

[20] Hermes, S., Witte, T., Hikov, T., Zacher, D., Bahnmu¨ller, S., Langstein, G., Huber, K., & Fischer, R. A. (2007). Trapping metal-organic framework nanocrystals: an in-situ time-resolved light scattering study on the crystal growth of MOF-5 in solution. *J. Am. Chem. Soc*., 129, 5324–5325. DOI: 10.1021/ja068835i

[21] Wang, Z., Wang, G., Qi, H., Wang, M., Wang, M., Park, S. W., Wang, H., Yu, M., Kaiser, U., Fery, A., Zhou, S., Dong, R., Feng, X. (2020). Ultrathin two-dimensional conjugated metal organic framework single-crystalline nanosheets enabled by surfactant-assisted synthesis. *Chem. Sci.*, 11, 7665. DOI: 10.1039/D0SC01408G

[22] Rodenas, T., Luz, I., Prieto, G., Seoane, B., Miro, H., Corma, A., Kapteijn, F., Llabre´s i Xamena, F.X., Gascon, J. (2015). Metal-organic framework nanosheets in polymer composite materials for gas separation. *Nat. Mater*., 14, 48–55. DOI: 10.1038/nmat4113

[23] Mahrunisa, N., Adawiah, A., Aziz, I., Zulys, A. (2023). Green synthesis of Cr-PTC-HIna metal organic frameworks (MOFs) and its application in methylene blue photocatalytic degradation. *Bulletin of Chemical Reaction Engineering & Catalysis*, 18(3), 362-374. DOI: 10.9767/bcrec.18885

[24] Zhao, M., Huang, Y., Peng, Y., Huang, Z., Ma, Q., Zhang, H. (2018). Two-dimensional metal-organic framework nanosheets: synthesis and applications. *Chem. Soc. Rev.*, 47, 6267–6295. DOI: 10.1039/C8CS00268A

[25] Yang, D.N., Geng, S., Zhang, H. (2024). Cu-MOF nanosheets with laccase-like activity for phenolic compounds detection and dye removal. *Inorganic Chemistry Communications*. 170, 113228. DOI: 10.1016/j.inoche.2024.113228

[26] He, C., Liu, C., Li, M., Li, M., Yin, J., Han, S., Xia, J., Chen, D., Cao, W., Lu, Q., Rosei, F. (2022). 3D hierarchical Cu-MOF nanosheets-based antibacterial mesh. *Chemical Engineering Journal*, 446, 137381. DOI: 10.1016/j.cej.2022.137381

[27] Shete, M., Kumara, P., Bachman, J.E., Ma, X., Smith, Z.P., Xu, W., Mkhoyana, K.A., Long, J.R., Tsapatsisa, M. (2018). On the direct synthesis of Cu(BDC) MOF nanosheets and their performance in mixed matrix membranes. *Journal of Membran Science*. 549, 312-320. DOI: 10.1016/j.memsci.2017.12.002

[28] Spingler, B., Schnidrig, S., Todorova, T., Wild, F. (2012). Some thoughts about the single crystal growth of small molecules. *CrystEngComm*, 14, 751–757. 123. DOI: 10.1039/C1CE05624G

[29] Elashery, S.E.A., Oh, H. (2021). Exploitation of 2D Cu-MOF nanosheets as a unique electroactive material for ultrasensitive Cu(II) ion estimation in various real samples. *Analytica Chimica Acta*. 1181, 338924. DOI: 10.1016/j.aca.2021.338924

[30] Sadjadi, S., Koohestani, F. (20222). Palladated composite of Cu-BDC MOF and perlite as an efficient catalyst for hydrogenation of nitroarenes. *Journal of Molecular Structure*, 1250 (171793). DOI: 10.1016/j.molstruc.2021.131793

[31] Mertsoy, E.Y. (2025). Energy-efficient synthesis of copper terephthalate metal–organic frameworks using sorbitol and choline chloride-based deep eutectic solvents for methylene blue removal. *Arabian Journal for Science and Engineering*, 1(1), 1–14. DOI: 10.1007/s13369-024-09890-x

[32] Zhan, G., Fan, L., Zhao, F., Huang, Z., Chen, B., Yang, X., Zhou, S.F. (2018). Fabrication of ultrathin 2D Cu-BDC nanosheets and the derived integrated MOF nanocomposites. *Adv. Funct. Mater*. 1806720. DOI: 10.1002/adfm.201806720

[33] Muttaqin, Hidayat, F.I. (2021). A Modest method of synthesis Cu- based metal-organic frameworks using benzene dicarbocxylate as a ligan for promising candidate of flue gas CO2 adsorption. *Jurnal Natural*, 21(3), 128–134. DOI: 10.24815/jn.v21i3.20035

[34] Sutapa, I.W., Palapessya, B.V., Souhoka, F.A., Bandjar, A. (2024). Synthesis of Cu-1,4-benzene dicarboxylate metal-organic frameworks (Cu-BDC MOFs) from plastic waste and its application as catalyst in biodiesel production. *Trends in Sciences*, 21(1), 2–15. DOI: 10.48048/tis.2023.7163

[35] Nayak, A., Viegas, S., Dasari, H., Sundarabal, N. (2022). Cu-BDC and Cu2O derived from Cu-BDC for the removal and oxidation of asphaltenes: a comparative study. *ACS Omega*, 7(39), 34966–34973. DOI: 10.1021/acsomega.2c03574

[36] Kormann, C., Bahnemann, D.W., Hoffmann, M. R. (1988). Photocatalytic production of hydrogen peroxides and organic peroxides in aqueous suspensions of titanium dioxide, zinc oxide, and desert sand. *Environmental Science & Technology*, 22(7), 798–806. DOI: 10.1021/es00172a009

[37] Hamdalla, T.A., Alfadhli, S., Khasim, S., Darwish, A.A.A., ElZaidia, E.F.M., Al-Ghamdi, S.A., Aljohani, M.M., Mahmoud, M.E., Seleim, S.M. (2024). Synthesis of novel Cu/Fe based benzene dicarboxylate (BDC) metal organic frameworks and investigations into their optical and electrochemical properties. *Heliyon*, 10(3), 1–13. DOI: 10.1016/j.heliyon.2024.e25065

[38] Xie, W., Liu, X.H., Wang, Y.X., Lai, W.H., Zhao, Q. (2023). Regulating the oxidation state of copper centers in metal-organic frameworks for enhanced carbon dioxide photoreduction. *Cell Reports Physical Science*, 4(10), 1–12. DOI: 10.1016/j.xcrp.2023.101587

[39] Yadav, R.S., Kuřitka, I., Vilcakova, J., Urbánek, P., Machovsky, M., Masař, M., Holek, M. (2017). Structural, magnetic, optical, dielectric, electrical and modulus spectroscopic characteristics of ZnFe2O4 spinel ferrite nanoparticles synthesized via honey-mediated sol-gel combustion method. *Journal of Physics and Chemistry of Solids*, 110(1), 87–99. DOI: 10.1016/j.jpcs.2017.05.029

[40] Dastbaz, A., Karimi-Sabet, J., Moosavian, M.A. (2019). Sonochemical synthesis of novel decorated graphene nanosheets with amine functional Cu-terephthalate MOF for hydrogen adsorption: effect of ultrasound and graphene content. *International Journal of Hydrogen Energy*. 44, 26444-26458. DOI: 10.1016/j.ijhydene.2019.08.116

[41] Wang, F., Guo, H., Chai, Y., Li, Y., Liu, C. (2013). The controlled regulation of morpholo gy and size of HKUST-1 by coordination mod ulation method. *Microporous and Mesoporous Materials*, 173, 181–188. DOI: 10.1016/j.micromeso.2013.02.023

[42] Nurbayti, S., Adawiah, A., Bale, U.F., Fadhilla, R., Ramadhan, F.N., Zulys, A., Sukandar, S., Saridewi, N., Tulhusna, L. (2024). Sonochemical assisted synthesis of Cr-PTC metal organic framework, ZnO, and Fe3O4 composite and their photocatalytic activity in methylene blue degradation. *Bulletin of Chemical Reaction Engineering & Catalysis*. 19(2), 318-326. DOI: 10.9767/bcrec.20156

[43] Adawiah, A., Luthfi, Y. M. D., Zulys, A. (2021). Photocatalytic Degradation of Methylene Blue and Methyl Orange by Y-PTC Metal-Organic Framework. *Jurnal Kimia Valensi*. 7(2), 129-141, DOI: 10.15408/jkv.v7i2.22267

[44] Zulys, A., Defania, M., Gunlazuardi, J., Adawiah, A., (2023) Glycine-modulated zirconium perylene-based metal-organic framework for rhodamin B photocatalytic degradation, *Molekul,* 18 (3), 497–507, DOI: 10.20884/1. jm.2023.18.3.91

[45] Hevira, L., Zilfa, Rahmayeni, Ighalo, J.O., Zein, R. (2020). Biosorption of indigo carmine from aqueous solution by Terminalia catappa shell. *Journal of Environmental Chemical Engineering*. 8(5), 1–11. DOI: 10.1016/j.jece.2020.104290

[46] Chen, X., Mao, S.S. (2007). Titanium dioxide nanomaterials: synthesis, properties, modifications, and applications. *Chemical Reviews*. 107(7), 2891–2959. DOI: 10.1021/cr0500535

[47] Saridewi, N., Utami, D.J., Zulys, A., Nurbayti, S., Nurhasni, Adawiah, Putri, A.R., Kamal, R. (2024). Utilization of Lidah mertua (Sansevieria trifasciata) extract for green synthesis of ZnFe2O4 nanoparticle as visible-light responsive photocatalyst for dye degradation. *Case Studies in Chemical and Environmental Engineering*. 9(2024) 100745. DOI: 10.1016/j.cscee.2024.100745

[48] Kumar, A., Pandey, G. (2017). A review on the factors affecting the photocatalytic degradation of hazardous materials. *Material Science & Engineering International Journal*. 1(3), 106–114. DOI: 10.15406/mseij.2017.01.00018

[49] Natarajan, S., Bajaj, H.C., Tayade, R.J. (2018). Recent advances based on the synergetic effect of adsorption for removal of dyes from waste water using photocatalytic process. *Journal of Environmental Sciences*. 65(3), 201–222. DOI: 10.1016/j.jes.2017.03.011

[50] Saridewi, N., Komala, S., Zulys, A., Nurbayti, S., Tulhusna, L., Adawiah, A. (2022). Synthesis of ZnO-Fe3O4 magnetic nanocomposites through sonochemical methods for methylene blue degradation. *Bulletin of Chemical Reaction Engineering & Catalysis*. 17(3), 650-660. DOI: 10.9767/bcrec.17.3.15492.650-660.